CA-MG-FE-RICH RHODONITE

from the

MORRO DA MINA MINE, CONSELHEIRO LAFAIETE, MINAS GERAIS, BRAZIL

Peter Leverett*, Peter A. Williams
School of Natural Sciences
University of Western Sydney
Locked Bag 1797
Penrith South DC NSW 1797, Australia

and

David E. Hibbs
School of Pharmacy
University of Sydney
NSW 2006, Australia

Large and superb crystals of translucent to gemmy, brilliant red rhodonite found in a manganese mine near Conselheiro Lafaiete, Brazil have been reaching the mineral market in recent years. The crystals have been analyzed and proved to be significantly enriched in calcium, magnesium and iron.

INTRODUCTION

The city of Conselheiro Lafaiete (20°40′S, 43°48′W) is located about 100 km south of Belo Horizonte in the interior of Minas Gerais, Brazil. It lies in the southern section of the Quadrilátero Ferrífero ("Iron Quadrangle"), a 7000 km² section of the São Francisco craton, characterized by Archean gneisses, Neoarchean greenstones and Paleoproterozoic sediments. The area around Conselheiro Lafaiete is part of the highly folded Barbacena Greenstone Belt, which has been intruded by a series of granodiorites and aplitic to pegmatitic dikes (Pires, 1977), and is host to a number of significant manganese deposits (Derby, 1901; Pires, 1977, 1983; Pires and Cabral, 2001).

The major mine in the district is the Morro da Mina open pit (opened in 1894), which produced some 12 million tons of oxide and silicate ore between 1902 and 1995 and is currently operated by Companhia Vale do Rio Doce. The deposit is characterized by rocks known as *gondites*, composed of quartz and spessartine, and *queluzites*, which are rich in spessartine, rhodonite, and rhodochrosite. Dominant primary manganese minerals include spessartine, tephroite, rhodonite, pyroxmangite, neotocite, bementite, Mn-rich cummingtonite, rhodochrosite and Mn-rich apatite (Pires, 1977, 1983).

*e-mail: p.leverett@uws.edu.au

Figure 1. Locality map.

Of particular interest to this study is a hydrothermally derived assemblage composed of spessartine, rhodonite and asbestiform Mn-rich cummingtonite (Pires, 1977). Recently, a considerable quantity of deep pink, gem-quality material supposed to be rhodonite from the Morro da Mina mine has appeared on the specimen market. The rhodonite is invested with varying amounts of cummingtonite needles, but some of the rhodonite is free of such inclusions.

Thomas Moore (in preparation), in his compendious Mineral Discoveries 1960–2010, writes of the occurrence as follows:

Rhodonite crystals "of gem quality" from Conselheiro Lafaiete, Minas Gerais have been reported as early as 1971. In the second half of the 1990's, a few specimens of rhodonite emerged from the Mn-rich, spessartine/amphibole/rhodonite/pyroxmangite skarn at Conselheiro Lafaiete; they are miniature-size, medium pink to pink-red aggregates of parallel, tightly intergrown, bladed crystals (reported in "What's new in minerals" in 1995 and 1999). Beginning around 2005, further work was done at the mine with a view to extracting rhodonite specimens from the Mn-rich skarn deposit, and at the 2006 Tucson Show a few fine rhodonite specimens were offered by an American dealer. They are thumbnails and miniatures, and two extraordinary specimens; one is a 5.2-cm cluster of gemmy, deep pink rhodonite crystals with a single, sharp individual measuring 2×3 cm; the other is a parallel group of two well-terminated crystals measuring 6 cm. These specimens are laboriously prepared by removing the hard mixture of amphibole, spessartine, and massive rhodonite/pyroxmangite from around the calcite-filled vugs which harbor the rhodonite crystals.

Both of the major specimens mentioned by Moore are pictured here.

Because of a question surrounding the true identity of the rhodonite specimens (Luiz Menezes, personal communication), we have investigated the material using a combination of electron microprobe, X-ray powder diffraction and single-crystal X-ray techniques. The study, results of which are reported below, has shown that the material in question is indeed a Ca-Mg-Fe-rich rhodonite.

EXPERIMENTAL

Crystals of rhodonite from the Morro da Mina mine were supplied by Luiz Menezes. A crystal fragment free of cummingtonite inclusions was embedded in epoxy resin, polished and carbon-coated. No zoning of the rhodonite was evident in BSE (back-scattered electron) images, but a single small inclusion some 30 μm across was noted. Five spot analyses of rhodonite and four of the inclusion were carried out using a Jeol 8600 electron microprobe (WDS mode, 30 kV, 20 nA, 3 μm beam diameter). Analytical data are given in Table 1. The empirical formula of the rhodonite based on 5 $(Si,Al)O_4$ groups is:

$$(Mn_{3.76}Ca_{0.50}Mg_{0.34}Fe_{0.33})_{\Sigma 4.93}(Si_{4.97}Al_{0.03})O_{15},$$
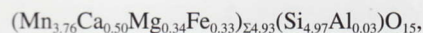
and the simplified formula normalized for an M^{2+} cation total of 5 pfu is:

$$(Mn_{3.81}Ca_{0.51}Mg_{0.35}Fe_{0.33})Si_5O_{15}.$$

The small inclusion has an empirical formula of:

$$(Mn_{3.69}Ca_{0.51}Fe_{0.33}Mg_{0.32})_{\Sigma 4.85}(Si_{4.97}Al_{0.03})O_{15},$$
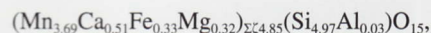

Figure 2. Rhodonite crystal with albite, 5.2 cm, from the Morro de Mina mine, Conselheiro Lafaiete, Minas Gerais, Brazil. Mike Bergmann specimen; Jeff Scovil photo.

Figure 3. Rhodonite, 6 cm, two terminated crystals in parallel growth from the Morro de Mina mine, Conselheiro Lafaiete, Minas Gerais, Brazil. Wayne Thompson and Jerry Romanilla specimen, now in a private collection; Jeff Scovil photo.

with the cation deficiency presumably accounted for by appropriate protonation of some of the silicate oxygen atoms. This phase was not studied further.

Powder X-ray diffraction data (Table 2) were recorded using a Philips PW1925-20 powder diffractometer (Cu Kα radiation, λ = 1.5406 Å, with pure Si as internal standard). For the single-crystal structure analysis, a cleavage fragment 0.45 × 0.45 × 0.30 mm in size was mounted on a Bruker SMART CCD diffractometer. A careful inspection of the reflection record showed that only one phase is present, i.e., the crystal used is free of inclusions. Unit cell dimensions were determined by least-squares refinement of the complete data set and are listed in Table 3 together with associated crystal data. All data were collected at 273(2) K using graphite-monochromatized Mo Kα radiation, corrected for Lorentz and polarization effects, and an absorption correction using SADABS was applied (Sheldrick, 1996). The structure was completely determined by direct methods using SHELXS (Sheldrick, 1997a) and refined on F^2 by full-matrix least-squares methods using SHELXL97 (Sheldrick, 1997b). All atoms were found to be in positions similar to the analogous atoms in the magnesian rhodonite reported by Peacor *et al.* (1978), and an initial isotropic refinement assuming all five metal sites were fully occupied by Mn gave $R1 = 0.051$ with no unusual thermal parameters. Allowing the five metal site occupancies to also vary at this stage reduced $R1$ to 0.037 and gave a good indication of the electron density present at each of the five metal sites. This was then used in conjunction with the electron microprobe analyses to deduce the probable distribution of Mn, Mg, Ca and Fe in each of

the sites, noting also the preference of the various different metal ions present to occupy these five non-equivalent metal sites (as discussed below) and the need to achieve acceptable thermal parameters for each site. A final anisotropic refinement of this distributed metal ion model resulted in most acceptable and nearly uniform U_{eq} values for each of the five metal sites and an $R1$ of 0.0242 and $wR2$ of 0.0646. The weighting scheme used was $w = 1/(\sigma^2 F_o^2 + 0.0364P^2 + 0.600P)$, where $P = (F_o^2 + 2F_c^2)/3$, as defined by SHELXL97 (Sheldrick 1997b). Crystal data and refinement details are given in Table 3. Final atomic parameters are listed in Table 4, anisotropic displacement parameters in Table 5, and selected bond lengths in Table 6.

RESULTS AND DISCUSSION

Analyses of rhodonite from the Morro da Mina mine (Table 1) are entirely consistent with the formulation of the mineral, with enrichment of Ca, Mg and Fe. Powder X-ray diffraction data listed in Table 2 are compared with those for an Mg-rich rhodonite from the Balmat mine No. 4, New York, USA, which has the composition $(Mn_{3.73}Mg_{0.73}Ca_{0.51}Fe_{0.03})Si_5O_{15}$ (Peacor *et al.*, 1978; JCPD File 83-2212). Powder X-ray data for rhodonite are quite sensitive to small variations in unit cell constants (Viswanathan and Harneit, 1986; Pinckney and Burnham, 1988), but those for the two cases above are very similar, due to the analogous Ca and Mg+Fe contents.

A number of studies have been directed towards understanding the distribution of cations among the five non-equivalent sites in rhodonite (Peacor and Niizeki, 1963; Dickson, 1975; Marshall and Runciman, 1975; Ohashi and Finger, 1975a,b; Peacor *et al.*, 1978; Nelson and Griffen 2005). It is clear that Ca substitutes in the M5 site, which is 7-coordinated and distorted. Fe distribution has been studied using Mössbauer spectroscopy (Dickson, 1975) and Fe(II) has been found to be present in all five sites, but not equally. Although Dickson (1975) was somewhat equivocal about the site preferences for Fe, it is evident that site occupancies for M1, M2 and M3 sites are approximately equal and M4 is slightly preferred; the M5 site is least preferred. Based on fitted intensities in the Mössbauer spectra at 77 K of a number of samples with varying Fe contents, the relative site occupancies for Fe in sites M1 to M5 are 0.67:0.67:0.67:1:0.24, respectively. We have distributed Fe in the present structure using the same regime, but note that with Mn dominant in sites M1 to M4 and almost equal to Ca in M5, the one-electron difference between Mn and Fe will have negligible bearing on the temperature factors, whatever the relative Fe:Mn distribution. Mg has been distributed over the five sites in the following way. For sites M1 to M3, sof values were assigned to give comparable $U(eq)$ values, and for M4 and M5 to account for the remainder in such a way as to mimic slightly higher relative $U(eq)$ values in line with the structure determination of Peacor *et al.* (1978). We cannot be absolutely certain of the sof values for Fe and Mg, but the structure refined sensibly and no anomalous patterns emerged in the anisotropic thermal parameters or the final difference map as a result of the adopted procedure.

There is no discrepancy in the structure as compared with others that have been reported for rhodonite (Peacor and Niizeki, 1963; Ohashi and Finger, 1975a,b; Peacor *et al.*, 1978; Pertlik and Zahiri, 1999; Nelson and Griffen 2005). In the present structure, and in line with the above reports, the M1, M2 and M3 sites are all quasi-octahedral, with the M4 site being somewhat more distorted to give a [5+1] coordination sphere (Table 6). The M5 site, which accommodates the larger Ca^{2+} ion, is 7-coordinated, with the usual [4+3] distribution of M-O bonds. Table 6 also indicates that the usual geometry of the silicate chain is present as evidenced by the Si-O bond lengths. For further structural details, the supplementary material should be consulted.

Table 1. Analytical data (wt%) for rhodonite and pyroxenoid inclusion.

Rhodonite	1	2	3	4	5	av.
MgO	2.06	1.97	2.58	2.03	1.99	2.13
Al_2O_3	0.45	0.59	0.47	0.46	0.49	0.49
SiO_2	46.94	46.45	46.77	47.01	47.01	46.84
CaO	4.45	4.32	4. 37	4.33	4.52	4.40
MnO	41.86	40.84	42.55	42.73	41.41	41.88
FeO	3.87	3.66	3.78	3.84	3.72	3.77
Total	99.63	97.83	100.52	100.40	99.14	99.50

Inclusion	1	2	3	4	av.
MgO	2.08	1.99	1.97	1.97	2.00
Al_2O_3	0.46	0.58	0.47	0.39	0.48
SiO_2	46.71	47.07	47.45	47.15	47.10
CaO	4.43	4.36	4.60	4.56	4.49
MnO	41.00	41.80	41.33	41.20	41.33
FeO	3.78	3.85	3.78	3.60	3.75
Total	98.46	99.65	99.60	98.87	99.15

Table 2. Powder X-ray diffraction data for rhodonite.

Morro da Mina[a]		Balmat mine No. 4[b]	
d_{obs}/Å	I_{rel}	d_{obs}/Å	I_{rel}
7.146	44	7.1	50
6.733	24	6.67	15
4.783	34	4.76	50
4.126	9	4.12	8
3.817	16	3.81	15
3.562	61	3.55	85
3.406	13	3.40	11
3.336	32		
3.255	15	3.25	12
3.138	58	3.13	76
3.091	89	3.08	100
2.970	100	2.969	100
2.927	50	2.925	63
2.805	16	2.809	10
2.783	22	2.781	26
2.759	26	2.748	46
2.651	16	2.648	18
2.597	39	2.593	34
2.540	11	2.535	7
2.513	55	2.505	65
2.452	10		
2.430	9	2.427	10
2.398	8	2.382	8
2.372	17	2.369	16
2.316	9	2.312	4
		2.259	3
2.223	68	2.220	24
		2.208	8
2.178	51	2.178	53
2.159	10	2.152	6
2.114	15	2.113	11
2.089	13	2.084	7
2.066	10	2.061	8
2.046	6		
1.980	10		
1.950	6	1.949	4
1.894	17	1.892	11
1.864	20	1.860	13
		1.831	7
plus 27 lines to 1.277			

[a]This work; $(Mn_{3.81}Ca_{0.51}Mg_{0.35}Fe_{0.33})Si_5O_{15}$.
[b]Peacor et al., 1978; $(Mn_{3.73}Mg_{0.73}Ca_{0.51}Fe_{0.03})Si_5O_{15}$.

Table 3. Crystal data and structure refinement details for rhodonite.

Empirical formula	$(Mn_{3.81}Ca_{0.51}Fe_{0.33}Mg_{0.35})Si_5O_{15}$
Formula weight	637.15
Temperature	273(2) K
Wavelength	0.71073 Å
Crystal system	Triclinic
Space group	$P\bar{1}$
Unit cell dimensions	$a = 6.6818(13)$ Å $\alpha = 105.49(3)°$
	$b = 7.6330(15)$ Å $\beta = 92.49(3)°$
	$c = 11.795(2)$ Å $\gamma = 94.01(3)°$
Volume	577.1(2) Å³
Z	2
Density (calculated)	3.667 Mg m⁻³
Absorption coefficient	5.341 mm⁻¹
F(000)	616
Crystal size	$0.45 \times 0.45 \times 0.45$ mm
θ range for data collection	1.80 to 28.62°
Index ranges	$-9 \leq h \leq 8, -9 \leq k \leq 9,$
	$-15 \leq l \leq 15$
Reflections collected	5685
Independent reflections	2675 [R(int) = 0.0184]
Completeness to θ = 28.62°	90.7%
Refinement method	Full-matrix least-squares on F^2
Data/restraints/parameters	2675/0/227
Goodness-of-fit on F^2	1.004
Final R indices [$I>2\sigma(I)$]	R1 = 0.0242, wR2 = 0.0623
R indices (all data)	R1 = 0.0286, wR2 = 0.0646
Extinction coefficient	0.0040(5)
Largest diff. peak and hole	0.491 and −0.533 e Å⁻³

Table 4. Atomic coordinates ($\times 10^4$), site occupancy factors (sof) and equivalent isotropic displacement parameters ($Å^2 \times 10^3$ for rhodonite. U(eq) is defined as one third of the trace of the orthogonalized U_{ij} tensor. All silicon and oxygen atom sites are fully occupied.

	x/a	y/b	z/c	sof	U(eq)
Mn(1)	1260(1)	3164(1)	4448(1)	0.88	6(1)
Mg(1)	1260(1)	3164(1)	4448(1)	0.05	6(1)
Fe(1)	1260(1)	3164(1)	4448(1)	0.07	6(1)
Mn(2)	−302(1)	8822(1)	8521(1)	0.89	6(1)
Mg(2)	−302(1)	8822(1)	8521(1)	0.04	6(1)
Fe(2)	−302(1)	8822(1)	8521(1)	0.07	6(1)
Mn(3)	1877(1)	5101(1)	7300(1)	0.87	6(1)

(continued on next page)

Table 4. (continued)

	x/a	y/b	z/c	sof	U(eq)
Mg(3)	1877(1)	5101(1)	7300(1)	0.06	6(1)
Fe(3)	1877(1)	5101(1)	7300(1)	0.07	6(1)
Mn(4)	2046(1)	7011(1)	10246(1)	0.75	7(1)
Mg(4)	2046(1)	7011(1)	10246(1)	0.15	7(1)
Fe(4)	2046(1)	7011(1)	10246(1)	0.10	7(1)
Mn(5)	3549(1)	−437(1)	3015(1)	0.42	10(1)
Ca(5)	3549(1)	−437(1)	3015(1)	0.51	10(1)
Fe(5)	3549(1)	−437(1)	3015(1)	0.02	10(1)
Mg(5)	3549(1)	−437(1)	3015(1)	0.05	10(1)
Si(1)	2938(1)	5420(1)	2626(1)		7(1)
Si(2)	3628(1)	7355(1)	5307(1)		6(1)
Si(3)	1537(1)	763(1)	6542(1)		6(1)
Si(4)	5038(1)	7814(1)	8751(1)		6(1)
Si(5)	2463(1)	12561(1)	9110(1)		7(1)
O(1)	1099(3)	2514(2)	6113(2)		8(1)
O(2)	1933(3)	5999(2)	5641(2)		9(1)
O(3)	396(3)	440(2)	3210(2)		8(1)
O(4)	1063(3)	4006(2)	2690(2)		8(1)
O(5)	577(3)	11579(2)	9603(2)		8(1)
O(6)	5161(3)	5794(2)	7797(2)		8(1)
O(7)	1926(3)	4525(2)	9025(2)		9(1)
O(8)	3767(3)	6832(2)	3885(2)		10(1)
O(9)	−3388(3)	9348(2)	8543(2)		8(1)
O(10)	4183(3)	2440(3)	4074(2)		15(1)
O(11)	2998(3)	1396(2)	7778(2)		9(1)
O(12)	5521(3)	7437(2)	10047(2)		8(1)
O(13)	2657(3)	8007(2)	8688(2)		8(1)
O(14)	2551(3)	6805(3)	11862(2)		12(1)
O(15)	2940(3)	9467(2)	5621(2)		12(1)

Table 5. Anisotropic displacement parameters ($\text{Å}^2 \times 10^3$) for rhodonite. The anisotropic displacement factor exponent takes the form $-2\pi^2[h^2a^{*2}U_{11} + ... + 2hka^*b^*U_{12}]$.

	U_{11}	U_{22}	U_{33}	U_{23}	U_{13}	U_{12}
M(1)	6(1)	7(1)	6(1)	1(1)	0(1)	0(1)
M(2)	5(1)	7(1)	6(1)	1(1)	0(1)	1(1)
M(3)	5(1)	6(1)	6(1)	1(1)	−1(1)	1(1)
M(4)	8(1)	9(1)	5(1)	2(1)	1(1)	4(1)
M(5)	9(1)	6(1)	15(1)	−1(1)	4(1)	−1(1)
Si(1)	6(1)	8(1)	6(1)	2(1)	1(1)	1(1)
Si(2)	6(1)	9(1)	5(1)	2(1)	0(1)	0(1)
Si(3)	6(1)	6(1)	6(1)	1(1)	0(1)	0(1)
Si(4)	5(1)	8(1)	6(1)	1(1)	0(1)	1(1)
Si(5)	6(1)	8(1)	6(1)	2(1)	0(1)	0(1)
O(1)	9(1)	8(1)	8(1)	3(1)	0(1)	1(1)
O(2)	9(1)	9(1)	8(1)	3(1)	1(1)	0(1)
O(3)	7(1)	9(1)	8(1)	2(1)	0(1)	−1(1)
O(4)	5(1)	9(1)	9(1)	2(1)	1(1)	1(1)
O(5)	7(1)	9(1)	8(1)	3(1)	1(1)	1(1)
O(6)	7(1)	9(1)	7(1)	0(1)	2(1)	0(1)
O(7)	10(1)	9(1)	9(1)	4(1)	−1(1)	1(1)
O(8)	11(1)	10(1)	7(1)	0(1)	1(1)	−2(1)
O(9)	8(1)	9(1)	8(1)	3(1)	1(1)	0(1)
O(10)	9(1)	27(1)	12(1)	10(1)	−1(1)	1(1)
O(11)	7(1)	10(1)	7(1)	1(1)	−1(1)	0(1)
O(12)	7(1)	10(1)	7(1)	3(1)	−1(1)	0(1)
O(13)	6(1)	8(1)	10(1)	3(1)	1(1)	1(1)
O(14)	11(1)	15(1)	11(1)	6(1)	−1(1)	2(1)
O(15)	14(1)	6(1)	16(1)	1(1)	8(1)	1(1)

Table 6. Selected bond lengths [Å] for rhodonite.

M(1)−O(10)	2.100(2)		M(2)−O(13)	2.130(2)
M(1)−O(1)	2.155(2)		M(2)−O(5)	2.175(2)
M(1)−O(3)	2.220(2)		M(2)−O(4)#1	2.257(2)
M(1)−O(2)	2.246(2)		M(2)−O(3)#1	2.258(2)
M(1)−O(2)#1	2.276(2)		M(2)−O(5)#2	2.327(2)
M(1)−O(4)	2.330(2)		Mn(2)−O(9)	2.128(2)
M(3)−O(1)	2.109(2)		M(4)−O(14)	1.971(2)
M(3)−O(4)#1	2.123(2)		M(4)−O(7)	2.046(2)
M(3)−O(7)	2.193(2)		M(4)−O(5)#2	2.110(2)
M(3)−O(6)	2.236(2)		M(4)−O(13)	2.211(2)
M(3)−O(2)	2.241(2)		M(4)−O(12)	2.352(2)
M(3)−O(13)	2.386(2)		M(4)−O(9)#2	2.827(2)
M(5)−O(9)#1	2.211(2)			
M(5)−O(14)#3	2.219(2)			
M(5)−O(10)	2.218(2)			
M(5)−O(3)	2.258(2)		Si(1)−O(14)#7	1.589(2)
M(5)−O(8)#4	2.568(2)		Si(1)−O(4)	1.614(2)
M(5)−O(11)#5	2.606(2)		Si(1)−O(8)	1.632(2)
M(5)−O(15)#6	2.727(2)		Si(1)−O(6)#6	1.641(2)
Si(2)−O(10)#5	1.585(2)		Si(3)−O(1)	1.591(2)
Si(2)−O(2)	1.613(2)		Si(3)−O(3)#9	1.614(2)
Si(2)−O(8)	1.626(2)		Si(3)−O(15)#4	1.638(2)
Si(2)−O(15)	1.657(2)		Si(3)−O(11)	1.657(2)
Si(4)−O(9)#10	1.594(2)		Si(5)−O(7)#8	1.594(2)
Si(4)−O(13)	1.609(2)		Si(5)−O(5)	1.628(2)
Si(4)−O(12)	1.652(2)		Si(5)−O(12)#11	1.639(2)
Si(4)−O(6)	1.657(2)		Si(5)−O(11)#8	1.654(2)

Symmetry transformations used to generate equivalent atoms are #1: $-x, -y+1, -z+1$; #2: $-x, -y+2, -z+2$; #3: $x, y-1, z-1$; #4: $x, y-1, z$; #5: $-x+1, -y, -z+1$; #6: $-x+1, -y+1, -z+1$; #7: $x, y, z-1$; #8: $x, y+1, z$; #9: $-x, -y, -z+1$; #10: $x+1, y, z$; #11: $-x+1, -y+2, -z+2$; #12: $x-1, y, z$.

SUPPLEMENTARY MATERIAL

Full lists of crystallographic data excluding structure factor tables have been deposited with the Inorganic Crystal Structure Database (ICSD), Fachinformationszentrum, Karlsruhe, Germany; CRYSDATA@FIZ-Karlsruhe.DE. Any request to the ICSD for this material should quote the full literature citation and the CSD number 418082. Lists of observed and calculated structure factors are available from the authors upon request.

REFERENCES

DERBY, O. A. (1901) On the manganese ore deposits of the Queluz (Lafayette) District, Minas Geraes, Brazil. *American Journal of Science*, 4th Series, **12**, 18–32.

DICKSON, B. L. (1975) The iron distribution in rhodonite. *American Mineralogist*, **60**, 98–104.

MARSHALL, M., and RUNCIMAN, W. A. (1975) The absorption spectrum of rhodonite. *American Mineralogist*, **60**, 88–97.

MOORE, T. P. (in preparation) *Mineral Discoveries 1960–2010.* To be published by the Mineralogical Record, Tucson.

NELSON, W. R., and GRIFFEN, D. T. (2005) Crystal chemistry of Zn-rich rhodonite ("fowlerite"). *American Mineralogist*, **90**, 969–983.

OHASHI, Y., and FINGER, L. W. (1975a) Pyroxenoids: a variation in chemistry of natural rhodonites and pyroxmangites. *Carnegie Institution of Washington, Year Book*, **74**, 561–564.

OHASHI, Y., and FINGER, L. W. (1975b) Pyroxenoids: a comparison of refined structures of rhodonite and pyroxmangite. *Carnegie Institution of Washington, Year Book*, **74**, 564–569.

PEACOR, D. R., and NIIZEKI, N. (1963) The redetermination and refinement of the crystal structure of rhodonite, $(Mn,Ca)SiO_3$. *Zeitschrift für Kristallographie*, **119**, 98–116.

PEACOR, D. R., ESSENE, E. J., BROWN, P. E., and WINTER, G. A. (1978) The crystal chemistry and petrogenesis of a magnesian rhodonite. *American Mineralogist*, **63**, 1137–1142.

PERTLIK, F., and ZAHIRI, R. (1999) Rhodonite with a low calcium content: crystal structure determination and crystal chemical calculations. *Monatshefte für Chemie*, **130**, 257–265.

PINCKNEY, L. R., and BURNHAM, C. W. (1988) Effects of compositional variation on the crystal structures of pyroxmangite and rhodonite. *American Mineralogist*, **73**, 798–808.

PIRES, F. R. M. (1977) *Geologia do Distrito Manganesífero de Conselheiro Lafaiete, Minas Gerais*. MSc Thesis, Universidade Federal do Rio de Janeiro.

PIRES, F. R. M. (1983) Manganese mineral parageneses in the Lafaiete District, Minas Gerais, Brazil. *Anais da Academia Brasileira de Ciências*, **55**, 272–285.

PIRES, F. R. M., and CABRAL, A. R. (2001). Estudos de Orville Derby sobre os depósitos manganesíferos do Brasil—edição comemorativa dos 150 anos de nascimento do cientista. *Revista Escola de Minas*, **54**, 205–209.

SHELDRICK, G. M. (1996) *SADABS. Empirical Absorption Correction Program for Area Detector Data*. University of Göttingen, Göttingen, Germany.

SHELDRICK, G. M. (1997a) *SHELXS97, A Program for the Solution of Crystal Structures*. University of Göttingen, Göttingen, Germany.

SHELDRICK, G. M. (1997b) *SHELXL97, A Program for the Refinement of Crystal Structures*. University of Göttingen, Göttingen, Germany.

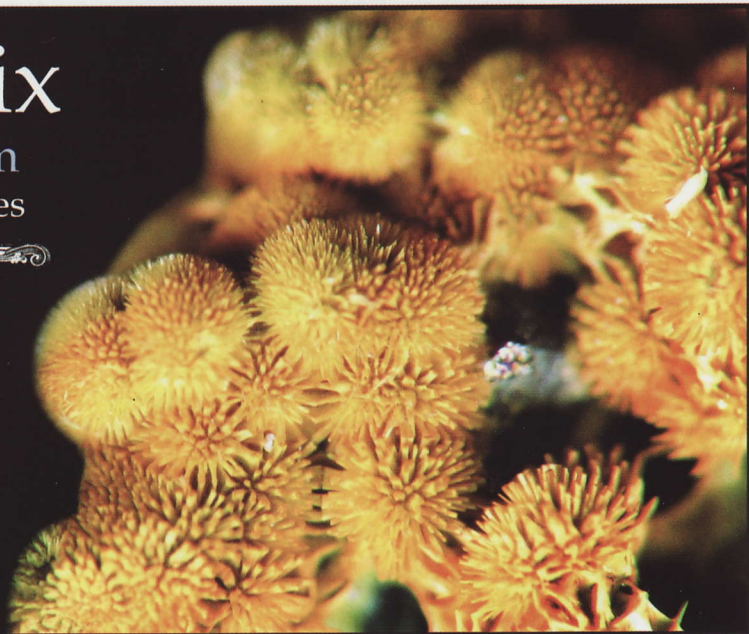VISWANATHAN, K., and HARNEIT, O. (1986) Lattice expansion and ionic substitution in common pyroxenoids. *Contributions to Mineralogy and Petrology*, **94**, 238–244. ⬙